



## Problem Statement

Autonomous modular robots are limited in individual capability and require connector mechanisms tolerating positional and angular misalignment.

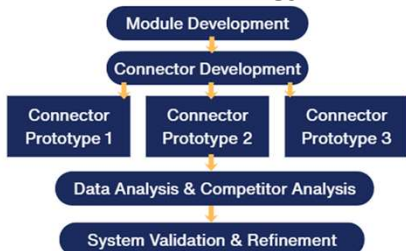
## Research Goal

Design and evaluate novel connector mechanisms that facilitates reliable autonomous self-assembly, targeting a soft robotic application.

## Graphical Abstract



## Methodology



## Background

- Modular robots are robots built from identical modules that connect and disconnect to reconfigure into different shapes.
- Magnetic Coupling:
  - Advantage: Errors in alignment
  - Disadvantage: Weak connect force
- Mechanical Coupling:
  - Strong connecting force
  - Requires precise aligning
- Multi-stage coupling mechanisms combine advantages of both magnetic and mechanical coupling
- Soft robots are deformable and can allow adaptive locomotion, a key advantage over many current modular robots.
- Soft and swarm robotic integration can provide key insights into the real-world application of self-assembly.

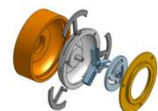
## Mechanical Designs

### Coupling Mechanisms



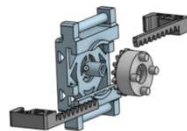
Prototype 1: Key Slot Connector

Uses a protruding key that slides into a matching slot. *Strengths:* provides a strong, rigid connection and is simple to manufacture. *Weaknesses:* gendered design requires specific orientation; alignment tolerance is poor, making docking difficult.



Prototype 2: Gendered Twist-Lock Connector

A bayonet or quarter-turn mechanism inspired by androgynous fasteners. *Strengths:* high versatility, high reliability, low orientation tolerance. *Weaknesses:* requires rotation during engagement; can be hard to align under load.



Prototype 3: Rack and Pinion Arm Grabber

A rack-and-pinion mechanism containing an arrangement where a rotating pinion gear meshes with a linear rack to convert rotation into controlled linear motion. *Strengths:* high strength, reversible engagement. *Weaknesses:* requires a certain extent of orientation reliance.

### Multi-axis Joint



Spherical Connector Joint

The round component is a bio-inspired multi-axis joint. Mimicking human shoulder movement, the ball-and-socket joint allows rotation about multiple axes from a single point. Connectors mounted on this joint can pivot freely in pitch, yaw, and roll, enabling modules to orient themselves for docking in any direction. The connecting joint has 360 degrees in yaw and 360 degrees in roll, allowing infinite rotational ability.

## Decision Matrix

| System             | Alignment | Strength | Reverse | Simplicity | Scale | Cost |
|--------------------|-----------|----------|---------|------------|-------|------|
| SMORES-EP          | 6         | 9        | 9       | 3          | 6     | 4    |
| M-Blocks           | 4         | 5        | 8       | 4          | 7     | 3    |
| Truss Links        | 2         | 3        | 2       | 5          | 3     | 5    |
| Soft Mag Connector | 8         | 4        | 9       | 7          | 8     | 9    |
| Prototype 1        | 6         | 6        | 3       | 4          | 6     | 10   |
| Prototype 2        | 7         | 7        | 5       | 5          | 3     | 10   |
| Prototype 3        | 8         | 10       | 9       | 6          | 4     | 10   |

Figure 8. Decision matrix comparing modular robotic connector systems and proposed prototypes across six engineering criteria. SMORES-EP (Liu et al., 2023), M-Blocks (Romanishin et al., 2015), Truss Links (Wyder et al., 2025), and a Soft Magnetic Connector (Tse et al., 2020) were evaluated on a 1–10 ordinal scale, with higher scores indicating better performance. Criteria include alignment tolerance, maximum strength, reversibility, simplicity, scalability, and relative cost. Cell shading is normalized within each criterion, where darker values indicate higher relative performance.

## Finite Element Analysis Simulation

### Von Mises Theory

Yielding begins when the distortional energy per unit volume equals that of a uniaxial tensile test at yield.

$$\sigma_{vm} = \sqrt{0.5[(\sigma_x - \sigma_y)^2 + (\sigma_y - \sigma_z)^2 + (\sigma_x - \sigma_z)^2] + 3(\tau_{xy}^2 + \tau_{yz}^2 + \tau_{zx}^2)}$$

where  $\sigma_x, \sigma_y,$  and  $\sigma_z$  are the normal stress values acting in the  $x, y,$  and  $z$  faces and  $\tau_{xy}, \tau_{yz},$  and  $\tau_{zx}$  are the shear stress values acting in the  $x, y,$  and  $z$  faces (Patei et al., 2019).

Finite element analysis numerically solves stress and deformation under applied loads, with von Mises stress serving as a failure-predictive metric for ductile materials.

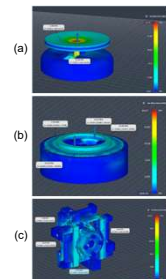


Figure 1: Finite element simulation of the connector under tensile load. The heatmap displays von Mises stress, highlighting peak stresses near the latch and reduced stress in the soft funnel. Simulating with ABS Plastic with ~45 Mpa of tensile force (ASTM International), connectors were tested until the breaking point. Stresses remain below material yield limits, validating structural integrity. (a) Prototype 1 withstood ~600 N of force before failure. (b) Prototype 2 withstood ~1.2 kN of force before failure. (c) Prototype 3 withstood ~4.8 kN of force before failure.

## AprilTag

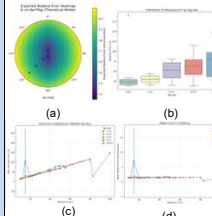


Figure 2: AprilTag pose estimation accuracy and error characterization across spatial position and distance.

## Analysis

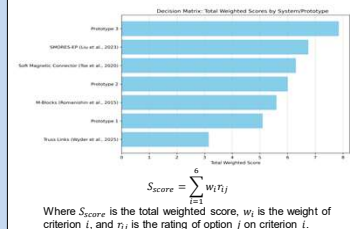


Figure 9. Weighted decision matrix for modular connector selection. Robustness (25%) and alignment tolerance (20%) were prioritized, with reversibility, simplicity, and scalability weighted at 15% each, and cost at 10%. Prototype 3 ranked highest (7.85) due to strong alignment, high strength, and low cost, followed by SMORES-EP (6.75) and the Soft Magnetic Connector (6.30).

$$S_{score} = \sum_{i=1}^6 w_i T_{ij}$$

Where  $S_{score}$  is the total weighted score,  $w_i$  is the weight of criterion  $i$ , and  $T_{ij}$  is the rating of option  $j$  on criterion  $i$ .

## Soft Robotic Module

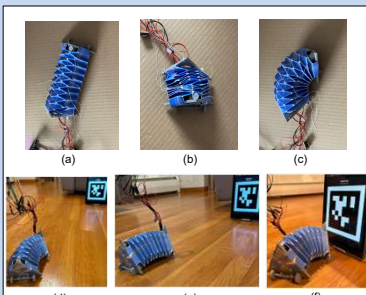


Figure 3: Physical demonstration of soft robotic module. (a) The module has a length of 170 mm when it is fully extended. (b) The fully compressed module has a length of 61 mm when it is fully compressed. (c) The maximum bending angle of the module is approximately 110 degrees. The maximum speed of the robot is about 10 cm/s. (d) The module approaching an AprilTag at t=2 seconds. (e) Module aligning to AprilTag at t=6 seconds. (f) Module aligning to AprilTag at t=13 seconds, achieving a distance of ~2.8 cm away.

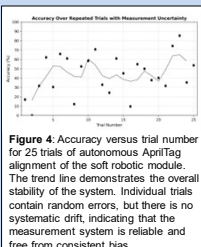


Figure 4: Accuracy versus trial number for 25 trials of autonomous AprilTag alignment of the soft robotic module. The trend line demonstrates the overall stability of the system. Individual trials contain random errors, but there is no systematic drift, indicating that the measurement system is reliable and free from consistent bias.



Figure 5: Robotic AprilTag detection flowchart (Richter et al., 2023).

AprilTag is a fiducial system using high-contrast tags in the shape of a square. Each tag contains a binary pattern that the detection algorithm can automatically identify and detection of a six-degree-of-freedom (x, y, z, roll, pitch, yaw) pose estimation from a single image.

## Systems Integration

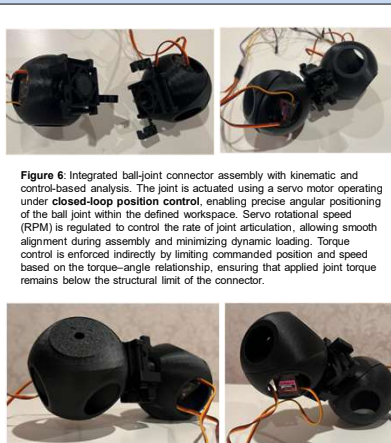


Figure 6: Integrated ball-joint connector assembly with kinematic and control-based analysis. The joint is actuated using a servo motor operating under closed-loop position control, enabling precise angular positioning of the ball joint within the defined workspace. Servo rotational speed (RPM) is regulated to control the rate of joint articulation, allowing smooth alignment during assembly and minimizing dynamic loading. Torque control is enforced indirectly by limiting commanded position and speed based on the torque-angle relationship, ensuring that applied joint torque remains below the structural limit of the connector.

### Yoshimura Fold Design

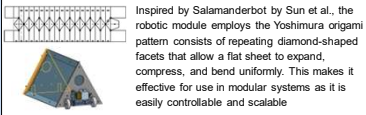


Figure 7: Mechanical characterization of the integrated ball-joint connector assembly during activation. Demonstration of kinematic lifting, in which one module lifts an adjacent module through controlled joint rotation, analogous to a single-link robotic arm actuated at the joint. During actuation, the joint maintains alignment under load while transmitting torque from the servo through the hybrid connector structure. This behavior demonstrates that the joint functions as a load-bearing, misalignment-tolerant robotic arm joint, capable of controlled lifting and positioning during modular robot assembly.

## Conclusions

- Prototype 3 achieved the strongest overall performance balance, driven by high load-bearing capacity, strong reversibility, and low projected manufacturing cost
- The results indicate that hybrid soft-mechanical connector designs can outperform purely magnetic or purely rigid approaches by combining misalignment tolerance with high mechanical strength
- Compared to existing state-of-the-art systems, the proposed designs exhibit improved scalability and projected cost efficiency, indicating feasibility for larger multi-module assemblies

## Future Work

- Investigate material substitutions and fabrication methods to further reduce cost while maintaining mechanical performance.
- Integrate AI-based vision systems to enable autonomous connector alignment and docking under uncertainty, using real-time perception to guide assembly decisions.
- Evaluate repeatability and wear behavior over extended connection cycles to assess long-term reliability and maintenance requirements.
- Optimize maximum allowable angular and translational offsets under which reliable connection can be achieved.

## References

ASTM International. ASTM D638–23 Standard test method for tensile properties of plastics. ASTM International. <https://www.astm.org/DOI10.1520/D638-23>

Liu, C., Lin, Q., Kim, H., & Yim, M. (2023). SMORES-EP: a modular robot with parallel self-assembly. *Autonomous Robots*, 47(2), 211–228. <https://doi.org/10.1007/s10544-022-10028-1>

Patei, R., Ribeiro, G., Thompson, D., Perkins, E., Hoover, J. J., Peters, J., & Tordesillas, A. (2019). A transdisciplinary approach for analyzing stress flow patterns in biostructures. *Mathematical and Computational Applications*, 24(2), 47. <https://doi.org/10.3390/mca2402047>

Richter, J., Böling, D., Nüchter, A., & Schilling, K. (2022). Advanced Edge Detection of AprilTags for Precise Docking Maneuvers of Mobile Robots. *IFAC-PapersOnLine*, 55(8), 117–123. <https://doi.org/10.1016/j.ifacol.2022.08.020>

Romanishin, J. W., Gilpin, K., Claici, S., & Rus, D. (2015). 3D M-Blocks: Self-reconfiguring robots capable of locomotion via pivoting in three dimensions. 2015 IEEE International Conference on Robotics and Automation (ICRA), 1925–1932. <https://doi.org/10.1109/ICRA.2015.7138450>

Sun, Y., Jiang, Y., Yang, H., Walter, L.-C., Santosio, J., Skornia, E. H., & Onal, C. (2020). SalamanderBot: A self-rigid composite continuum mobile robot for traversing complex environments. 2020 IEEE International Conference on Robotics and Automation (ICRA), 2953–2959. <https://doi.org/10.1109/ICRA40945.2020.9198790>

Tse, Y. A., Liu, S., Yang, Y., & Wang, M. Y. (2020). A Flexible Connector for Soft Modular Robots Based on Micropatterned Interference Jamming. 2020 3rd IEEE International Conference on Soft Robotics (RoboSoft), 150–155. <https://doi.org/10.1109/RoboSoft4309.2020.919975>

Wyder, P. M., Bakhshi, R., Zhao, M., Booth, D. A., Modi, M. E., Song, A., Kang, S., Wu, J., Patel, P., Kasuri, R. T., Yi, D., Garg, N. N., Jungjurnwala, P., Bhutania, S., Tong, E. H., Xu, Y., Griedler, J., Mustafa, O., Kim, D., & Lipson, H. (2020). Robot metabolism: Toward machines that can grow by consuming other machines. *Science Advances*, 11(29). <https://doi.org/10.1126/sciadv.abb6887>